



**HAL**  
open science

## Spontaneous magnetization in dipolar needles

George Miloshevich, Thierry Dauxois, Ramaz Khomeriki, S. Ruffo

► **To cite this version:**

George Miloshevich, Thierry Dauxois, Ramaz Khomeriki, S. Ruffo. Spontaneous magnetization in dipolar needles. 2013. hal-00825128v1

**HAL Id: hal-00825128**

**<https://hal.science/hal-00825128v1>**

Preprint submitted on 23 May 2013 (v1), last revised 23 Aug 2013 (v2)

**HAL** is a multi-disciplinary open access archive for the deposit and dissemination of scientific research documents, whether they are published or not. The documents may come from teaching and research institutions in France or abroad, or from public or private research centers.

L'archive ouverte pluridisciplinaire **HAL**, est destinée au dépôt et à la diffusion de documents scientifiques de niveau recherche, publiés ou non, émanant des établissements d'enseignement et de recherche français ou étrangers, des laboratoires publics ou privés.

# Spontaneous magnetization in dipolar needles

George Miloshevich<sup>1,2</sup>, Thierry Dauxois<sup>3</sup>, Ramaz Khomeriki<sup>1,4</sup>, Stefano Ruffo<sup>3,5</sup>

<sup>(1)</sup> *Department of Physics, Faculty of Exact and Natural Sciences, Tbilisi State University, 0128 Tbilisi, Georgia*

<sup>(2)</sup> *Department of Physics, The University of Texas at Austin, Austin TX 78712, USA*

<sup>(3)</sup> *Laboratoire de Physique de l'Ecole Normale Supérieure de Lyon, Université de Lyon and CNRS, 46, allée d'Italie, F-69007 Lyon, France*

<sup>(4)</sup> *Max-Planck Institute for the Physics of Complex Systems, Nöthnitzer Str. 38, 01187 Dresden, Germany*

<sup>(5)</sup> *Dipartimento di Fisica e Astronomia and CSDC, Università di Firenze, CNISM and INFN, via G. Sansone, 1, Sesto Fiorentino, Italy*

(Dated: May 23, 2013)

Needle shaped three-dimensional classical spin systems with purely dipolar interactions have been studied in the microcanonical ensemble, with both numerical simulations and analytical approximations. We have observed spontaneous magnetization for different finite cubic lattices. The transition from the paramagnetic to the ferromagnetic phase is first order, and for two lattice types we have observed magnetization flips near the transition region. We explain these effects by mapping the model Hamiltonian to a one-dimensional Ising model with competing antiferromagnetic nearest neighbor and ferromagnetic mean-field interactions. This could be among the few, if not the first, experimentally testable prediction of the exotic properties of long-range interacting systems.

PACS numbers: 75.10.Hk; 05.70.Fh; 05.70.-a; 64.60.Cn

Systems with long-range interactions are of fundamental and practical interest because of their exotic statistical properties such as ensemble inequivalence, negative specific heat, temperature jumps, ergodicity breaking, etc. [1] Recently, a number of mean-field type models have been developed which are very convenient for analytical understanding [2, 3]. However, up to now, the connection to real physical systems has not been seriously addressed [4–6].

Dipolar force is one of the best candidates for experimental and theoretical studies of long-range interactions [7]. For instance, experimental studies have been performed on layered spin structures [8]. For these systems, intralayer exchange is much larger than the interlayer one: hence, every layer can be identified as a single macroscopic spin. As a consequence, dipolar forces between layers are dominant and one can describe the system with an effective long-range one-dimensional model [5]. However, in order to perform a careful study of the statistical properties of such samples, one should simulate the spins in each layer taking into account quantum effects, which is computationally heavy.

Alternatively, one can consider purely dipolar systems known as dipolar ferromagnets [9] where dipolar effects prevail over short-range exchange interactions. It has been pointed out long before [10] that body centered cubic (bcc) or face centered cubic (fcc) needle like samples should display spontaneous magnetization, while primitive cubic centered (pcc) could be ordered only antiferromagnetically. On the other hand, it was later argued that dipolar systems cannot show nonzero magnetization in the thermodynamic limit [11]. All these theoretical studies were performed within the canonical ensemble. Since we know that ensemble inequivalence is expected also for dipolar systems, it is important to perform a study in the

microcanonical ensemble.

In this Letter, we study by numerical simulations and analytical approximations the microcanonical dynamics of dipolar needles. We want to check if such systems can display spontaneous magnetization and study the time evolution of magnetization near the phase transition. This dynamics has been previously observed experimentally on short-range dipolar samples, showing features of telegraph noise [12].

Systems of classical spins with only dipolar interactions are described by the following Hamiltonian

$$\mathcal{H} = \frac{1}{2} \sum_{i \neq j} \frac{1}{r_{ij}^3} \left( \vec{S}_i \cdot \vec{S}_j - 3 \frac{(\vec{S}_i \cdot \vec{r}_{ij})(\vec{S}_j \cdot \vec{r}_{ij})}{r_{ij}^2} \right) \quad (1)$$

where  $|\vec{S}_i| = 1$  is a unit vector located at the  $i$ -th lattice site and  $\vec{r}_{ij}$  is the displacement vector between  $i$ -th and  $j$ -th site. The time evolution of  $\vec{S}_i$  is described by the following torque equation

$$\frac{d\vec{S}_i}{dt} = \vec{S}_i \times \vec{H}_i \quad \text{where} \quad \vec{H}_i = -\frac{\partial \mathcal{H}}{\partial \vec{S}_i}. \quad (2)$$

Here,  $\vec{H}_i$  is the local magnetic field acting on the spin attached to the  $i$ -th lattice site. In order to compare with experiments, the evolution of real spins can be recovered from Eq. (2) by redefining  $\vec{S}_i \rightarrow \sigma \vec{S}_i$  ( $\sigma$  stands for a spin length) and rescaling the time variable  $t \rightarrow 2\mu_B^2 \sigma^2 t$  ( $\mu_B$  is a Bohr magneton).

In numerical experiments, we solve the torque equation (2) for spins on pcc, bcc and fcc lattices shown in Fig. 1. Initially, the spins are aligned along the main axis of the sample as shown in the figure. In the course of time, we monitor all the three components of the average magnetization  $\vec{m} = (1/N) \sum_{i=1}^N \vec{S}_i$ , where  $N$  is the number of spins over which we perform an average.

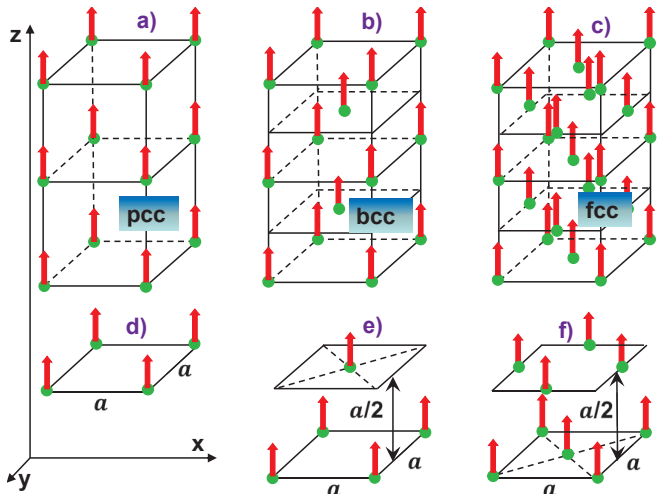


FIG. 1: Simple needle-like samples considered for numerical simulations. Graphs a), b) and c) graphs show the distribution of the spins in primitive centered (pcc), body centered (bcc) and face centered (fcc) cubic lattices, respectively. In graphs d), e) and f), an enlarged view of the spin positions in close transversal  $xy$ -layers is displayed. The arrows indicate the initial direction of the spins while  $a$  is the lattice spacing.

While for numerical simulations we directly use Hamiltonian (1) with the torque equation (2), our analytical approach is based on heuristic approximations by which we are able to map the main properties of Hamiltonian (1) to those of the simple one-dimensional mean-field model studied in Ref. [3].

We consider samples elongated in the  $z$ -direction. This is the ordering direction of the spin system because the demagnetizing field is smaller along this axis. For simplicity, we neglect the transversal components of the spin vectors, only the longitudinal components  $S_i^z$  are considered. As a further simplification, we assume that the longitudinal component takes only two values  $S_i^z = \pm 1$ , i.e. we reduce to Ising spins. After making such a crucial simplification, we follow the standard treatment in Refs. [13, 14]. The sums in Hamiltonian (1) are divided into two parts: The first part is the sum restricted only to a neighborhood of a site, the second part is the sum over the remaining portion of the sample. We treat this latter sum, which takes into account the long-range character of the dipolar interaction, via a continuum approximation. As far as we consider only the  $z$  components of the spins, it is easy to see that, for all considered lattices, in each layer transversal to the  $z$ -component of the sample, the coupling among the spins is antiferromagnetic. On the contrary, the coupling between neighboring spins in close transversal layers is ferromagnetic. This latter contribution will be included in the ferromagnetic type couplings appearing in the sum over the remaining part of the sample which is treated with a continuum approximation. Using these approximations and assuming that the sample is ellipsoidal, we can reduce Hamiltonian (1)

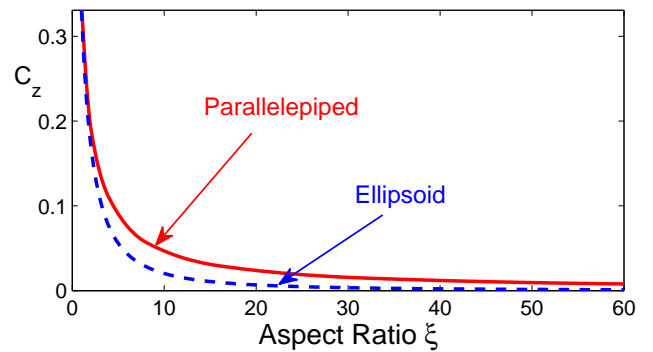


FIG. 2: Demagnetizing coefficient  $C_z$  computed numerically for a parallelepiped using formula (5) (solid line) versus the aspect ratio of the needle. We also plot the exact curve for an ellipsoid (dashed line) whose expression is given in formula (6).

to the following effective Hamiltonian

$$\mathcal{H}_{eff} = -\frac{K}{2} \sum_{\langle i, i' \rangle} (S_i^z S_{i'}^z - 1) - \frac{J}{2N} \left( \sum_{i=1}^N S_i^z \right)^2, \quad (3)$$

where  $\langle i, i' \rangle$  means that the sum is restricted only to nearest neighbors in the transversal layers.

The ferromagnetic mean-field coupling constant  $J$  can be computed in the continuum approximation, giving the following expression

$$J = \frac{4\pi(1 - 3C_z)}{3v_0}, \quad (4)$$

where  $v_0$  is the volume per spin while the demagnetizing factor  $C_z$  is given by the following integral [14]

$$C_z = -\frac{1}{4\pi V} \int_V d^3r \int_V d^3r_1 r_1 \frac{\partial^2}{\partial z^2} \left( \frac{1}{|\vec{r} - \vec{r}_1|} \right), \quad (5)$$

where  $V$  is a volume of the sample.

The demagnetizing coefficient  $C_z$  is  $1/3$  if the sample length  $L$  coincides with the lattice spacing  $a$ , while it tends to zero if the aspect ratio  $\xi = (L + a)/2a$  tends to infinity. In Fig. 2, we plot the dependence of this coefficient on the aspect ratio, comparing the case of a parallelepiped with that of an ellipsoid for which the exact expression is

$$C_z^{ell} = \frac{1 - b^2}{2b^3} \left( \ln \frac{1 + b}{1 - b} - 2b \right), \quad (6)$$

where  $b = \sqrt{1 - 1/\xi^2}$ .

Let us remark that the second term in the effective Hamiltonian (3) contains the  $z$ -component of the average magnetization  $m_z = (1/N) \sum_{i=1}^N S_i^z$ , and its typical size can be varied by changing the aspect ratio  $\xi$ , i.e. the length  $L$  of the sample.

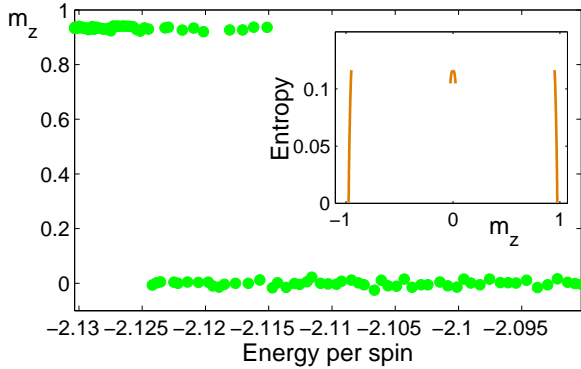


FIG. 3: Final values of the  $z$ -component of the magnetization  $m_z$  versus energy per spin, obtained in numerical simulations of the pcc lattice in Fig. 1a and 1d. In the inset, we plot entropy versus magnetization of the effective Hamiltonian (3) at a typical energy in the range of the transition.

We emphasize that the effective Hamiltonian (3) is the same as that in formula (1) of Ref. [3]. In the following, we will use results obtained for this Hamiltonian to discuss the phase diagram of model (1). Our approach consists in performing an estimate of the values of the couplings  $K$  and  $J$  based on features of the finite sample. In Ref. [3], it is proven that Hamiltonians of type (3) undergo a phase transition of the ferromagnetic type. This phase transition is second order if both couplings  $K$  and  $J$  are positive. It becomes first order if the coupling  $K$  is sufficiently negative, which favors locally the antiferromagnetic phase. The phase transition is present for values above  $K/J = -0.5$ , while for values below, the system is always in the paramagnetic phase. Hence, what determines the presence of the phase transition in model (1) is the ratio  $K/J$ . This ratio can be estimated using the above expression of  $J$  for particular choices of the lattice (e.g. those of Fig. 1) and by a rough estimate of the coupling constant  $K$ .

For the *primitive cubic lattices* in Fig. 1a and 1d which has four spins in the transversal layer, the coupling constant  $K = -2/a^3$ . For  $\xi \rightarrow \infty$ , Eq. (5) leads to  $J = 4\pi/(3a^3)$ , since the volume per spin in a pcc lattice is  $v_0 = a^3$ . Thus,  $K/J = -3/(2\pi) > -0.5$  and, therefore, we can expect the presence of a ferromagnetic phase.

In order to verify this prediction, we have performed numerical simulations of model (1), on a  $2 \times 2 \times 50$  pcc lattice, starting from a fully magnetized initial state, i.e. all spins pointing strictly along the  $z$ -axis. We then vary the energy of the initial state by adding random transversal components to the spins. We let the system relax towards a stationary state (this typically happens at times of the order  $10^4$ ) and monitor the final value of  $m_z$  for each value of the energy. We checked that the final state does not contain domains by looking at the spatial patterns of the individual spins. Collecting all these final values of

the magnetization, we plot them as a function of energy per spin in Fig. 3. We clearly observe a jump in magnetization from a positive value to zero and the presence of a coexistence region, where both a paramagnetic and a ferromagnetic phase are present, in full accordance with the predictions of the effective Hamiltonian (3). For symmetry reasons, we should have observed also the negative magnetization state if we had prepared the sample with the spins aligned opposite to the  $z$ -axis. The existence of this symmetry is confirmed by looking at the entropy of the effective Hamiltonian (3) (see Eq. (3) in [3]) as a function of  $m_z$ , shown in the inset of Fig. 3. The first order phase transition takes place when the maxima of the entropy of the paramagnetic and ferromagnetic states are at the same height.

As we vary the size and the shape of the sample, the couplings  $K$  and  $J$  in Hamiltonian (1) change. We have then to check whether we are still in a region of parameters where the phase transition is present. It happens that for a pcc lattice, an increase of the base size cancels the phase transition and the system always remains in the paramagnetic phase. Indeed for a wider base, each spin has four neighbors and thus the effective antiferromagnetic coupling constant  $K = -4/a^3$ , while the ferromagnetic mean-field constant remains  $J = 4\pi/(3a^3)$  even for large aspect ratios. Therefore the ratio  $K/J \approx -1$  does not allow for magnetized states to exist. This has been verified in numerical simulations which show that, even in the case of a  $3 \times 3$  base, there is no phase transition.

In order to verify whether other types of lattices support phase transitions as suggested in [10], we have performed simulations for bcc and fcc lattices shown in graphs b), c), e) and f) in Fig. 1. We have shown that these lattices do have a phase transition if the aspect ratio is large enough, and therefore these dipolar samples display spontaneous magnetization.

For *body centered cubic lattices*, we have four spins in a layer and one spin in the neighboring layer. In the layer with four spins, the situation is exactly the same as that of the pcc lattices, while in the layer with one spin there is no intralayer interaction. Thus, 4/5 of all spins can be treated as in pcc lattices, while one of the five cannot have an antiferromagnetic coupling. This latter spins forms a vertical chain, and their contribution to the Hamiltonian is a simple energy shift. Thus, the effective Hamiltonian for this lattice takes the form

$$\mathcal{H}_{eff}^{bcc} = \frac{4}{5}\mathcal{H}_{eff} + \frac{1}{5}NE_0. \quad (7)$$

The antiferromagnetic coupling constant  $K$  is unchanged. On the contrary, the mean-field ferromagnetic coupling constant  $J$  changes and can be calculated from Eq. (4). The average volume per spin is now  $v_0 = 4a^3/5$ , which implies that for large aspect ratios  $J = 5\pi/(3a^3)$ . As a consequence,  $K/J \approx -0.4$  and we can therefore expect from what we know of Hamiltonian (3), many dif-

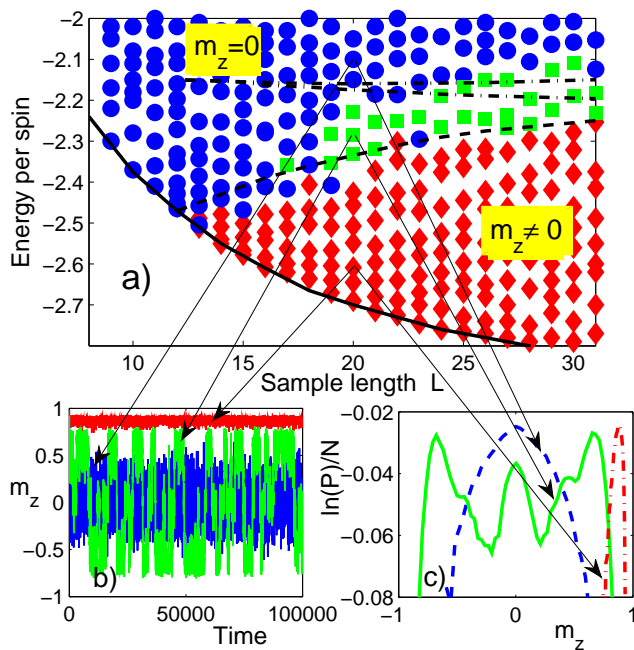


FIG. 4: a) Phase diagram of Hamiltonian (1) for the bcc lattice in Figs. 1b and 1d. Circles (blue), diamonds (red) and squares (green) represent ferromagnetic, paramagnetic and flipping states, respectively. The solid line is the minimal energy computed using Hamiltonian (7), the dashed one is the phase transition line and the dash-dotted lines are the bounds of the region with magnetization flips, again computed with the same effective Hamiltonian. b) Time evolution of the magnetization in different energy regions as shown by the arrows:  $L = 20$  with an energy per spin  $-2.6$  (ferromagnetic),  $-2.3$  (flips) and  $-2.1$  (paramagnetic). c) Entropy per spin for the three phases in panel b).

ferent regimes, contrary to the case of the pcc lattices where the ratio  $K/J$  is close to  $-0.5$ .

In the following, we will need an estimate of the value of the energy shift  $E_0$ . Two ferromagnetic contributions appear in this quantity: the first one comes from the sum over all the sample while the second one derives from the sum over the neighboring spins along the vertical chain. For large aspect ratios, one has approximately  $E_0 = [-5\pi/(3a^3) - 4/a^3]/2$ .

We have performed numerical simulations for the bcc lattice of the full dipolar Hamiltonian (1). We have first concentrated our attention on detecting the presence of a phase transition. As control parameters, we use the energy per spin and the length  $L$  of the sample. In Fig. 4a, we plot with circles the paramagnetic states and with diamonds the ferromagnetic ones. The dashed line separating ferromagnetic from paramagnetic states is obtained from the effective Hamiltonian (7) confirming the reliability of our analytical approach. The minimal energy for each sample length is also calculable from Hamiltonian (7) and is shown by the solid line in Fig. 4a: the agreement with numerical simulations of Hamiltonian (1)

is also very good. The effective Hamiltonian also predicts an intermediate region between the two phases, where magnetization  $m_z$  flips among positive, negative and zero values. This region is delimited by the dash-dotted lines in Fig. 4a. Numerical simulations confirm the presence of a region of magnetization flips as shown in Fig. 4b, but not precisely at the same location in the parameter space. In Fig. 4c, we plot for three different energies the entropy per spin  $s = (\ln P(m_z))/N$  where  $P(m_z)$  is obtained from the histogram of the magnetization. The first energy is in the paramagnetic phase and the entropy correctly shows a single hump centered around zero magnetization. A second energy is in the region of flips and the entropy shows three peaks, one centered in zero and two symmetric ones centered at positive and negative values of the magnetization. Finally, a third energy in the ferromagnetic phase shows a single peak at a positive value of the magnetization. Like for pcc lattices, we have checked whether the phase transition persists if one increases the size of the base of the bcc lattice. With four spins in the transversal layers, we get  $K/J = -3/(2\pi) > -0.5$ , which predicts that magnetized states can be realized in the bcc lattice even for large bases and for large aspect ratios.

Finally, let us switch to *face centered cubic lattices*. In the simplest realization of this lattice, there are four and five spins in subsequent transversal layers (see Figs. 1c and 1f). Numerical simulations show the same phenomenology as the one of bcc lattices, for the smaller lengths. However, by looking at the effective Hamiltonian for this lattice, we can predict that, like for the pcc lattice, magnetization does not persist for larger bases. Indeed, each spin interacts with four neighbors inside a transversal layers and thus the antiferromagnetic coupling constant  $K = -8\sqrt{2}/a^3$ . The volume per spin is  $v_0 = a^3/4$  and therefore  $J = 16\pi/(3a^3)$  for large bases and large aspect ratios. Consequently,  $K/J = -3/(\sqrt{2}\pi) < -0.5$ , which excludes the presence of spontaneous magnetization.

As the length of the sample increases the system becomes more and more one-dimensional. One might therefore doubt the existence of spontaneous magnetization for large aspect ratios, because dipolar force is short-range in one dimension. However, it is well known that one dimensional systems, although they do not spontaneously magnetize, they have a diverging correlation length at small temperatures,  $\ell = \exp(2g/T)$ , where  $g$  is the short-range coupling constant and  $T$  is temperature. We would like to give an estimate of this correlation length to compare it with the sample lengths that we use. First of all, one can get an estimate of the temperature by treating canonically the single spin in interaction with the thermal bath of all other spins. In the mean-field approximation [15],  $m_z = \tanh[H/T]$  where  $H = (K + J)m_z$  is assumed to be constant over the whole lattice. In our simulations for bcc lattices, the minimal magnetization

for which the ferromagnetic state survives is in the range  $m_z \simeq 0.65$ . Using the mean-field formula above, we get the approximate value of the temperature of the system:  $T \simeq 2$ . The corresponding short-range coupling constant is  $g = (K + J)/2$ , from which we get the value of the correlation length  $\ell \approx 3$ . This value is much smaller than the typical length of the sample, and then we can conclude that the magnetization that we observe is not of short-range origin.

In conclusion, we have shown clear evidences of the presence of spontaneous magnetization in needle-like samples, within the microcanonical ensemble. We believe that the origin of this effect is the long-range character of Hamiltonian (1), which we were able to map onto an effective one-dimensional Ising model with competing antiferromagnetic short range and ferromagnetic mean-field couplings. The presence of jumps in magnetization as energy is varied, the coexistence of paramagnetic and ferromagnetic phases in some energy ranges, and the presence of flips of magnetization in time are all indications that the phase transition we observe is of the first order. We have simulated three different kinds of cubic lattices and all of them show spontaneous magnetization in some parameter ranges. Flips are found only for bcc and fcc lattices. Magnetization flips which have features of telegraph noise have been observed experimentally for short-range ferromagnet [12]. It could be extremely interesting to check experimentally the presence of similar flips in the purely dipolar samples described in Ref. [9]. This could be among the few, if not the first, evidence of the exotic properties of long-range interacting systems.

We thank B. Barbara and D. Mukamel for helpful discussions. This work has been partially supported by the joint grant EDC25019 from CNRS (France) and SRNSF (Georgia) and also by the grant LORIS (ANR-10-CEXC-010-01). Numerical simulations were done at PSMN, ENS-Lyon. R. Kh. is supported by the grant No 30/12

from SRNSF.

- 
- [1] A. Campa, T. Dauxois, S. Ruffo, *Physics Reports* **480**, 57 (2009).
  - [2] J. Barré, D. Mukamel, S. Ruffo, *Phys. Rev. Lett.* **87**, 030601 (2001).
  - [3] D. Mukamel, S. Ruffo, N. Schreiber, *Phys. Rev. Lett.* **95**, 240604 (2005).
  - [4] M. Chalony, J. Barré, B. Marcos, A. Olivetti, D. Wilkowski, *Phys. Rev. A* **87**, 013401 (2013).
  - [5] A. Campa, R. Khomeriki, D. Mukamel, S. Ruffo, *Phys. Rev. B* **76**, 064415 (2007).
  - [6] R. Bachelard, T. Manos, P. de Buyl, F. Staniscia, F.S. Cataliotti, G. De Ninno, D. Fanelli, N. Piovella, *Journal of Statistical Mechanics-Theory and Experiment* **P06009** (2010).
  - [7] D. Mukamel, in *Long-Range Interacting Systems*, T. Dauxois, S. Ruffo and L. Cugliandolo (Eds.), Oxford University Press, Ch. 1, p. 33 (2009); S.T. Bramwell, *ibid*, Ch. 17, p. 549.
  - [8] M. Sato, A. J. Sievers, *Nature* **432**, 486 (2004).
  - [9] P. Beauvillan, J.-P. Renard, I. Laursen, P.J. Walker, *Phys. Rev. B* **18**, 3360 (1978); M.R. Roser, L.R. Corruccini, *Phys. Rev. Lett.* **65**, 1064 (1990); A. Biltmo, P. Henelius, *Europhys. Lett.* **87**, 27007 (2009).
  - [10] J. M. Luttinger, L. Tisza, *Phys. Rev.* **70**, 954 (1946); **72**, 257 (1947).
  - [11] R. B. Griffiths, *Phys. Rev.* **176**, 655 (1968).
  - [12] W. Wernsdorfer, E.B. Orozco, K. Hasselbach, A. Benoit, B. Barbara, N. Demoncy, A. Loiseau, H. Pascard, D. Maily, *Phys. Rev. Lett.* **78**, 1791 (1997).
  - [13] L.D. Landau, E.M. Lifshits, *Course of Theoretical Physics, Vol. 8: Electrodynamics of Continuous Media*, London, Pergamon (1960).
  - [14] A.I. Akhiezer, V.G. Baryakhtar, S.V. Peletminskij, *Spin Waves*, Amsterdam, North Holland (1968).
  - [15] A. Abragam, M. Goldman, *Nuclear Magnetism: Order and Disorder*, Clarendon Press, Oxford (1982).